

# Sintering parameters influence on dielectric properties of modified nano-BaTiO<sub>3</sub> ceramics

## Aleksandar Stajcic\*

Center of Microelectronic Technologies, Institute of Chemistry,
Technology and Metallurgy-National Institute of the Republic of Serbia,
University of Belgrade, Belgrade, Serbia
stajcic@nanosys.ihtm.bg.ac.rs

#### Ivana Stajcic

Department of Physical Chemistry, VINCA Institute of Nuclear Sciences, National Institute of the Republic of Serbia, University of Belgrade, Belgrade, Serbia ivana\_r@vinca.rs

#### Vojislav V. Mitic

Faculty of Electronic Engineering, University of Nis, Nis, Serbia;
Institute of Technical Sciences of SASA, University of Belgrade, Belgrade, Serbia
vmitic.d2480@qmail.com

### Chun-An Lu

Material and Chemical Research Laboratories (MCL), Industrial Technology Research Institute of Taiwan, ITRI, Taiwan luchunan@itri.org.tw

#### Branislav Vlahovic

Department of Physics, Centers for Research Excellence in Science and Technology, North Carolina Central University (NCCU), Durham, NC, USA vlahovic@nccu.edu

#### Dana Vasiljevic-Radovic

Center of Microelectronic Technologies, Institute of Chemistry, Technology and Metallurgy-National Institute of the Republic of Serbia, University of Belgrade, Belgrade, Serbia dana@nanosys.ihtm.bg.ac.rs

> Received 11 January 2022 Revised 1 March 2022 Accepted 7 March 2022 Published 2 July 2022

<sup>\*</sup>Corresponding authors.

BaTiO<sub>3</sub> (BTO) is considered the most commonly used ceramic material in multilayer ceramic capacitors due to its desirable dielectric properties. Considering that the miniaturization of electronic devices represents an expanding field of research, modification of BTO has been performed to increase dielectric constant and DC bias characteristic/sensitivity. This research presents the effect of N<sub>2</sub> and air atmospheres on morphological and dielectric properties of BTO nanoparticles modified with organometallic salt at sintering temperatures of 1200°C, 1250°C, 1300°C, and 1350°C. Measured dielectric constants were up to 35,000, with achieved very high values in both atmospheres. Field emission scanning electron microscopy (FESEM) was used for morphological characterization, revealing a porous structure in all the samples. The software image analysis of FESEM images showed a connection between particle and pore size distribution, as well as porosity. Based on the data from the image analysis, the prediction of dielectric properties in relation to morphology indicated that yttrium-based organometallic salt reduced oxygen vacancy generation in N<sub>2</sub> atmosphere. DC bias sensitivity measurements showed that samples with higher dielectric constant had more pronounced sensitivity to voltage change, but most of the samples were stable up to 100 V, making our modified BTO a promising candidate for capacitors.

Keywords: Dielectric properties; sintering; image analysis; nanoceramics modification; capacitors.

#### 1. Introduction

In recent years, research and development around the world have become oriented towards renewable energy sources due to a possible deficit of petroleum and coal in the future, and the greenhouse effect produced by the excessive use of their derivatives. 1-4 These problems pose an important environmental challenge, thus, making any possible solution attractive for a thorough investigation to speed up the route to potential industrial applications. The efficiency and quality of energy storage devices are evaluated by their energy and power density. <sup>5</sup> Ceramic materials are used for the production of high-temperature resistant capacitors, known for their good power density.<sup>6</sup> Among them, perovskite-type ceramics emerged as dielectric materials with the highest potential for use in capacitors due to their high dielectric constant and chemical resistance. <sup>7,8</sup> Barium titanate–BTO (BaTiO<sub>3</sub>) is a perovskite with excellent dielectric, ferroelectric, and piezoelectric properties. Therefore, it has been employed in capacitors for a long time.<sup>9-14</sup> The synthesis of BTO is well researched, resulting in various approaches, from sintering at high temperatures towards hydrothermal synthesis at lower temperatures. 15-18 All of these pathways gave BTO with different particle sizes, from micrometers to nanometers, which enabled BTO to satisfy the need for miniaturization of electronic devices. Efficient miniaturization led to the production of small-sized multilayer ceramic capacitors (MLCCs) with high capacitance value and stability due to the possibility of stacking thin layers of dielectrics and controlling their interface. 19,20 However, during MLCC processing, performed under the reducing atmosphere conditions, BTO powder is liable to generate oxygen vacancies, which can easily increase the conductivity of the overall ceramic, thereby reducing the pressure resistance and reliability of the product.<sup>21–24</sup> Furthermore, better insulation resistance caused by vacancies leads to a lower dielectric constant, which greatly reduces the capacitance of MLCCs. As an

answer to this challenge, the doping of BTO with rare earth elements and their oxides is usually performed and extensively studied so far.<sup>25–31</sup> When rare earth oxides are added, permanent electron–hole pairs are generated in the structure. This effect can greatly increase the dielectric strength of the material under the action of the electric field, resulting in better reliability of the MLCCs. Theoretically, as a result of doping, the ceramic internal structure forms a core-shell structure. The shell layer is a BTO layer doped with a rare earth oxide or modified additive, which has good insulation resistance and high voltage resistance characteristics while the core layer maintains a relatively pure crystal structure of BTO. Keeping the material with high dielectric properties as a core could also maintain good DC Bias characteristics. However, considering that dielectric constant and DC bias stability depend on the grain size, the desirable dopant would increase the former while reducing the latter.<sup>32</sup>

The focus of this research was on BTO surface modification using organometallic salt, with the aim of producing high dielectric constant material for ceramic capacitors. The influence of different particle sizes and sintering temperatures on dielectric properties was investigated to determine the most beneficial modification processing parameters. A core-shell structure was expected with yttrium-organic salt as an outer layer and BTO as an inner layer. In addition, morphological properties of samples were used to predict dielectric constant, depending on the porosity and pore size distribution. The findings gave an interesting insight into dielectric properties changes, important for the development of MLCCs and the future miniaturization of electronic devices.

### 2. Experimental

The manufacturer of BaTiO<sub>3</sub> (BTO) nanoparticles was Sakai Chemical Industry Co., Ltd., Sakai, Osaka, Japan. A yttrium-carboxylate salt was used for the coating of the core material BTO. Particles with three different diameter size distributions were used for the coating process.

To compare dielectric and morphological properties obtained under different processing conditions, sintering was performed in the air and N<sub>2</sub> atmosphere separately. Figure 1 presents a detailed coating and sintering process, which was performed at 1200°C, 1250°C, 1300°C, and 1350°C in air and at 1200°C, 1250°C, and 1300°C in N<sub>2</sub>. Modified samples were labeled according to their size and sintering atmosphere. BTO1MA, BTO2MA, and BTO3MA stand for samples modified in air, while BTO1MN, BTO2MN, and BTO3MN represent those modified in the nitrogen atmosphere.

The morphology of the coated BTO sintered in different atmospheres was investigated using scanning electron microscopy (EmCraft cube 2). Energy-dispersive X-ray analysis (EDX) using the Cliff-Lorimer method with all the elements analyzed (normalized) was used to establish the homogeneity and composition of samples. Purchased BTO particle size distribution presented in Fig. 2 and in Table 1 was

### A. Stajcic et al.

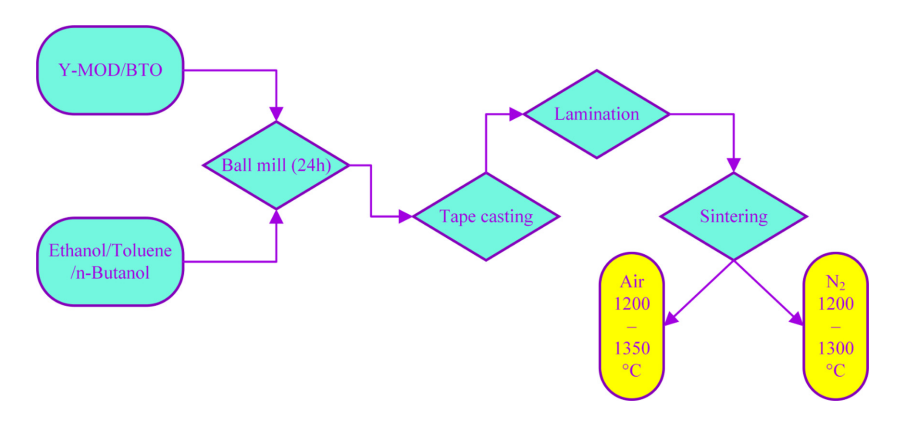


Fig. 1. (Color online) Schematic diagram of BTO coating and sintering process.

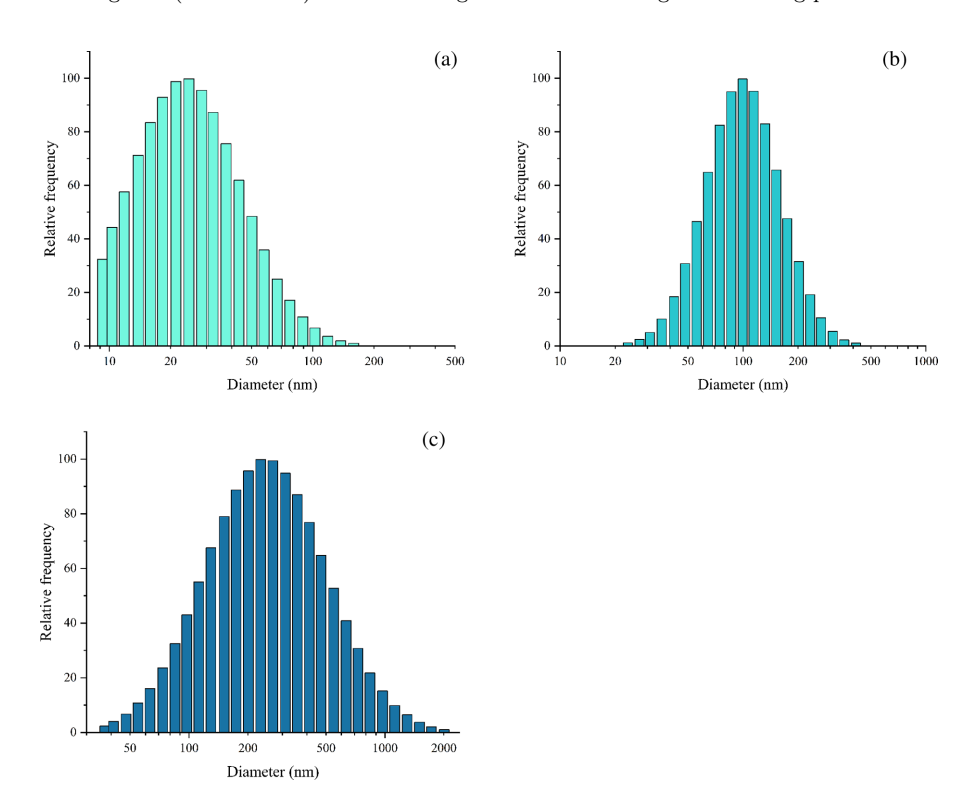


Fig. 2. (Color online) Size distribution for particles: (a) BTO1; (b) BTO2; (c) BTO3.

obtained using Nicomp 380 DLS/ZLS Dynamic Light Scattering and Zeta Potential. Dielectric constant values were measured using Microtest LCR Meter 6377@1 KHz, while KEITHLEY 2400 SourceMeter was used for capacitance change with the applied voltage (DC bias). All the measurements were performed at room temperature (25°C).

Table 1. Diameter size distribution for unmodified BTO particles.

	BTO1	BTO2	ВТОЗ
Mean diameter, nm	28.6	111.2	316.3
50% of distribution $<$ nm	25.3	99.5	246.5
90% of distribution $< nm$	55.0	181.9	612.7

### 3. Results and Discussion

## 3.1. Morphological and compositional analysis

Samples sintered at 1300°C were chosen for after-sintering morphology comparison, depending on the starting particle size (BTO1M, BTO2M, and BTO3M) and the sintering atmosphere (air or nitrogen). The occurrence common for all the samples is the disappearance of visible grain boundary (Figs. 3 and 4), caused by the liquid phase formation during high-temperature sintering. The liquid phase leads to the densification of a structure giving compact ceramics with expected good dielectric properties.

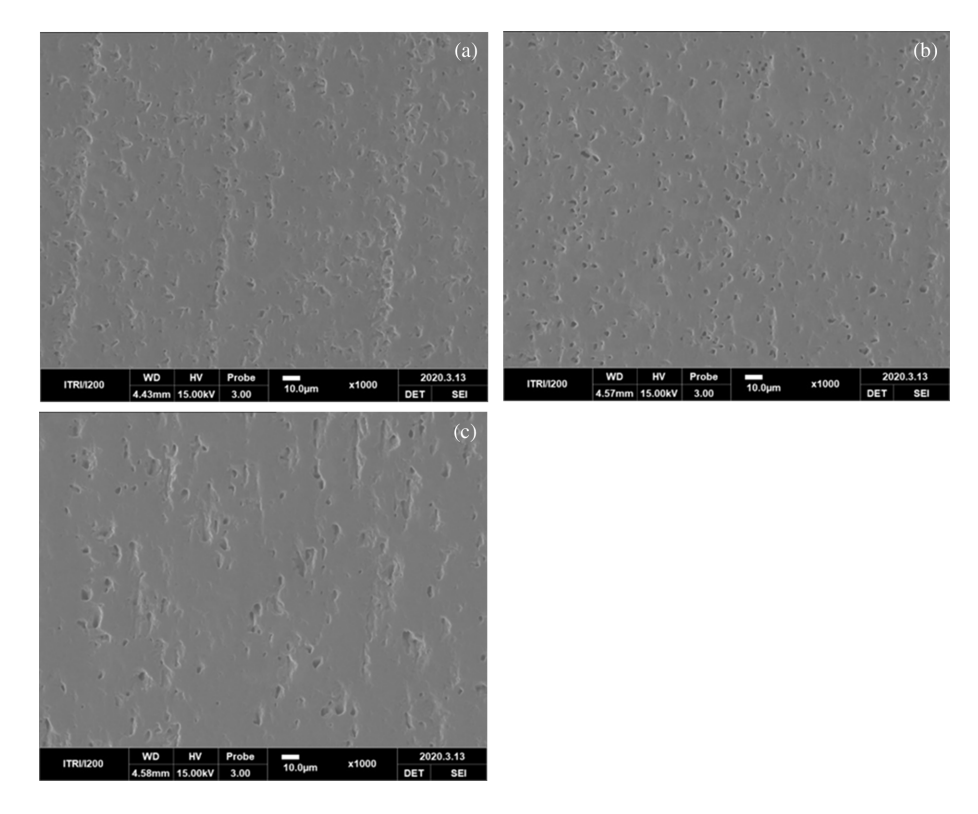


Fig. 3. FESEM of BTO1MA, BTO2MA, and BTO3MA sintered at 1300°C.

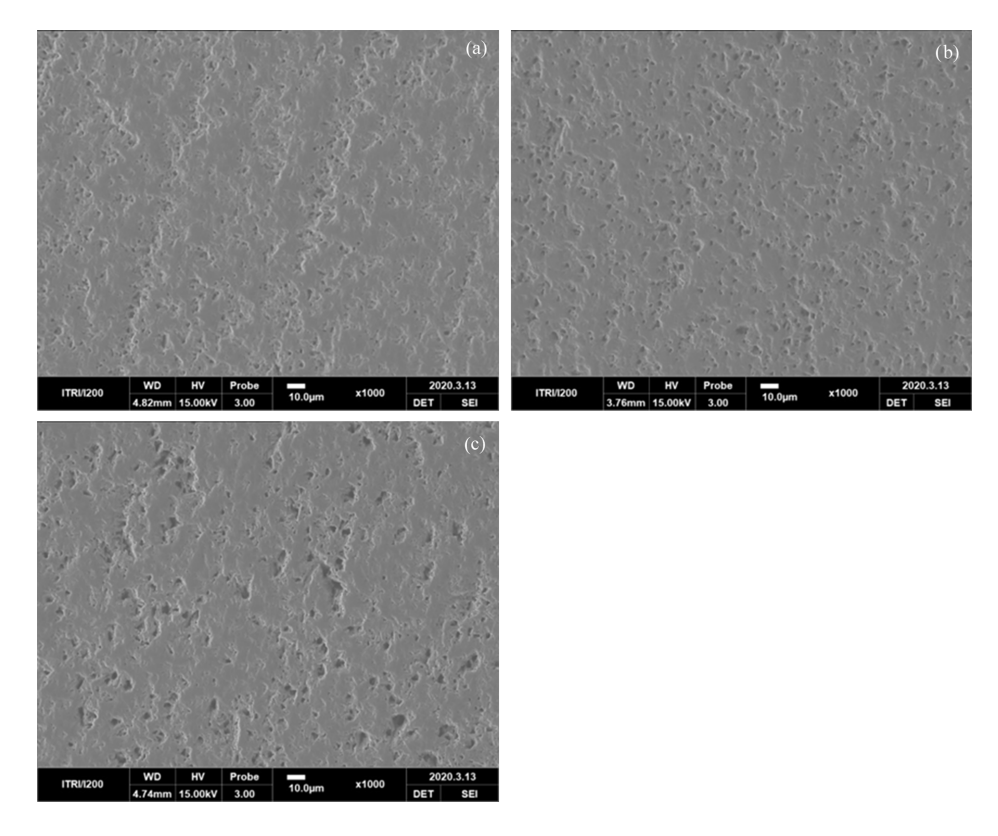


Fig. 4. FESEM of BTO1MN, BTO2MN, and BTO3MN sintered at 1300°C.

However, pore formation in all of the samples indicated that undesired volatilization occurred during sintering.<sup>34</sup> Pore size distribution and porosity can influence greatly dielectric constant, causing a substantial decrease. For more thorough morphology investigation, software image analysis was used, giving perception on particle size-porosity-pore size connections.

Pore size distribution has been presented through relative frequency and pore count, revealing that the particle size of unmodified BTO dictates the pore size of modified samples (Fig. 5 and Table 2). The main reason for this dependence is a larger-surfaced area in smaller particles that allows efficient modification with organometallic salts and the formation of more compact morphology. Furthermore, larger particles were more prone to the formation of pore clusters during sintering (Table 2). The relative frequency has provided an insight into a fraction of different pore size ranges (Fig. 5(a)) but pore count revealed that there was a great difference in the number of formed pores between samples (Fig. 5(b)) which strongly influenced overall porosity. The highest number of pores was identified in the BTO2MA sample, which amounted to a porosity nearly three times higher than that of the BTO1MA sample that presumably causes a decrease in the dielectric constant.

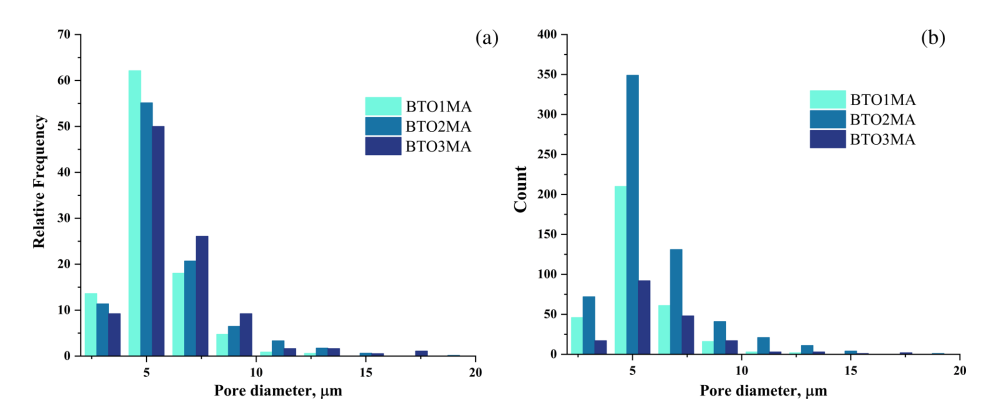


Fig. 5. (Color online) Pore size distribution for samples sintered in air presented via: (a) relative frequency; (b) number of pores.

Table 2. Image analysis results for a BTO-modified series in air atmosphere.

Sample	Pore diameters $\leq 5$ $\mu m$ , %	Mean pore diameter, $\mu$ m	Single pores/clusters, %/%	Porosity, %
BTO1MA	75	5.35	86/14	12.77
BTO2MA	66	5.93	81/19	33.60
BTO3MA	59	6.12	71/29	9.39

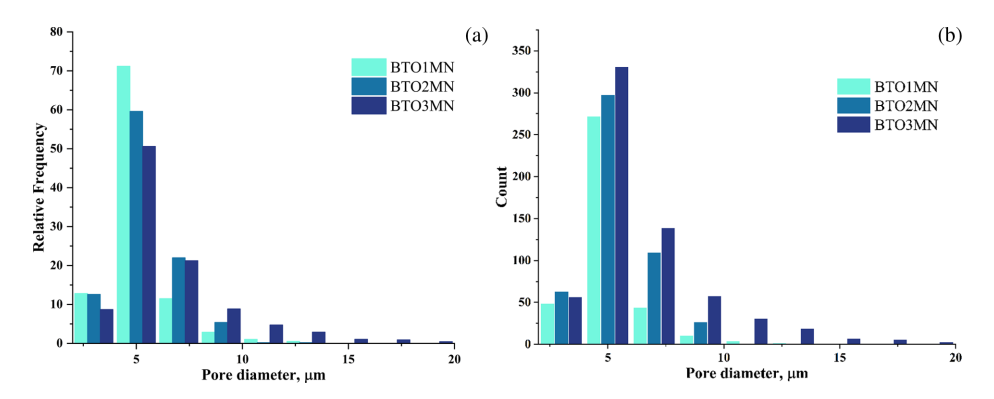


Fig. 6. (Color online) Pore size distribution for samples sintered in  $N_2$  presented through: (a) relative frequency; (b) number of pores.

As opposed to this, even with the largest pore diameters, the BTO3MA sample showed the lowest porosity because of a low pore count on the sample surface.

A similar trend was observed in  $N_2$  with the difference in higher pore count and porosity in all of the samples, which indicates more pronounced volatilization and atom migration in reducing atmosphere (Fig. 6 and Table 3). With the porosity higher than 40%, BTO3MN is expected to have poor dielectric properties compared to the rest of the samples.<sup>35</sup>

Sample	Pore diameters $\leq 5$ $\mu m$ , %	Mean pore diameter, $\mu$ m	Single pores/clusters, %/%	Porosity, %
BTO1MN	84	5.58	80/20	26.20
BTO2MN	72	6.00	80/20	23.70
BTO3MN	59	6.46	70/30	43.87

Table 3. Image analysis results for a BTO-modified series in N<sub>2</sub> atmosphere.

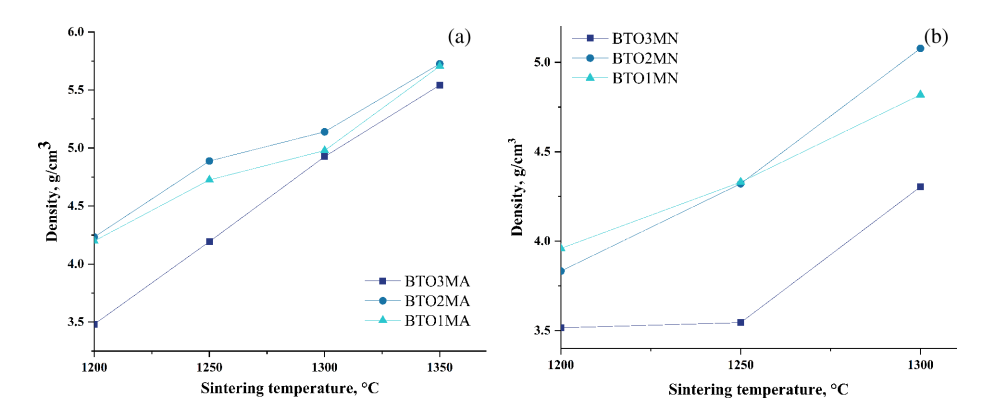


Fig. 7. (Color online) Density values of BTO samples modified in: (a) air; (b) N<sub>2</sub>.

## 3.2. Density

During sintering in nitrogen, residual carbon is to be expected at grain boundaries, inhibiting grain growth, which should further lead to higher densification, i.e. lower porosity.  $^{36,37}$  Nitrogen reducing atmosphere is known to promote oxygen vacancy generation, thus, causing poor dielectric properties. In addition, a high concentration of vacancies leads to a dense microstructure with lower porosity. In our case, samples sintered in air showed lower porosity compared to those modified in  $N_2$ , but similar density values (Fig. 7), indicating that BTO modification with Yttrium organic salt diminished oxygen vacancy formation in reducing atmosphere, presumably increasing the dielectric constant  $(D_k)$  of the material, while higher porosity could induce its decrease. Dielectric measurements were used to investigate which phenomenon had a stronger impact on  $D_k$  and DC bias sensitivity.

## 3.3. Dielectric properties

#### 3.3.1. Dielectric constant

Samples sintered in both nitrogen and air at 1200°C and 1250°C show similar dielectric constant values, except for BTO1M in nitrogen at 1250°C (3767), which is around two times higher compared to all of the other samples in both atmospheres (Fig. 8). It has been shown in earlier researches that porosity can increase in certain ceramics during sintering above 1200°C, as well as the grain growth, as a

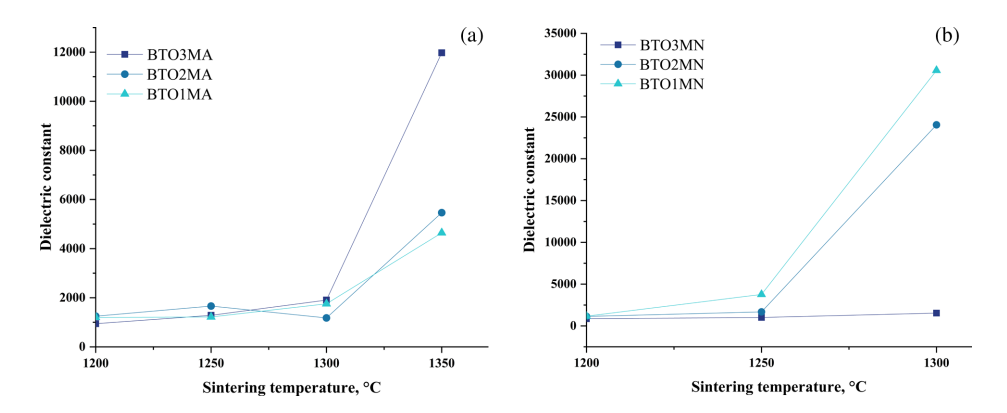


Fig. 8. (Color online) Dielectric constant values for BTO samples sintered in: (a) air; (b) N2.

consequence of the grain boundary atoms migration. 37 At 1300°C, the influence of the sintering atmosphere and the modifying agent is by far more pronounced. As assumed in density analysis, higher porosity in nitrogen indicates that successful modification diminished oxygen vacancy generation. Although the porosity of the samples modified in nitrogen at 1300°C can be considered high, the resulting effect is a sharp rise in dielectric constant for all the samples. According to image analysis results, samples BTO1MN and BTO2MN sintered at 1300°C were expected to show higher dielectric constant values compared to BTO3MN, which was confirmed with dielectric measurements (Fig. 8(b)). In the last sample, influence of nearly 50% porosity prevailed, leading to a dielectric constant of around 1540, which is by the order of magnitude lower compared to the former two samples. The value of 30572 for BTO1MN is considered exceptionally high, making it an excellent candidate for future investigations of grain boundary dielectric properties. For comparison, samples sintered in air at 1300°C had  $D_k$  below 2000 (Fig. 8(b)), which is typical for BaTiO<sub>3</sub> measured at room temperature (25°C).<sup>38</sup> As expected after the software image analysis, BTO2MA had the lowest  $D_k$  value (1178) due to the highest porosity (Table 2). When observing overall dielectric constant values, it must be emphasized that dielectric measurements were performed at the room temperature of 25°C, far below the Curie point of BTO, where the dielectric constant reaches the maximum value. A sharp rise in  $D_k$  appeared with the samples sintered in air at 1350°C, where BTO3MA reached the value of 11975. Considering that the predictions made after the morphological image analysis proved to be correct, it can be assumed that low porosity of the BTO3MA sintered at 1350°C played a key role in the  $D_k$  increase, which will be the subject of our future research.

### 3.3.2. DC bias sensitivity

The reverse of the spontaneous polarization in perovskite ceramics is a well-known phenomenon.<sup>39</sup> Without the influence of externally applied voltage, barium titanate

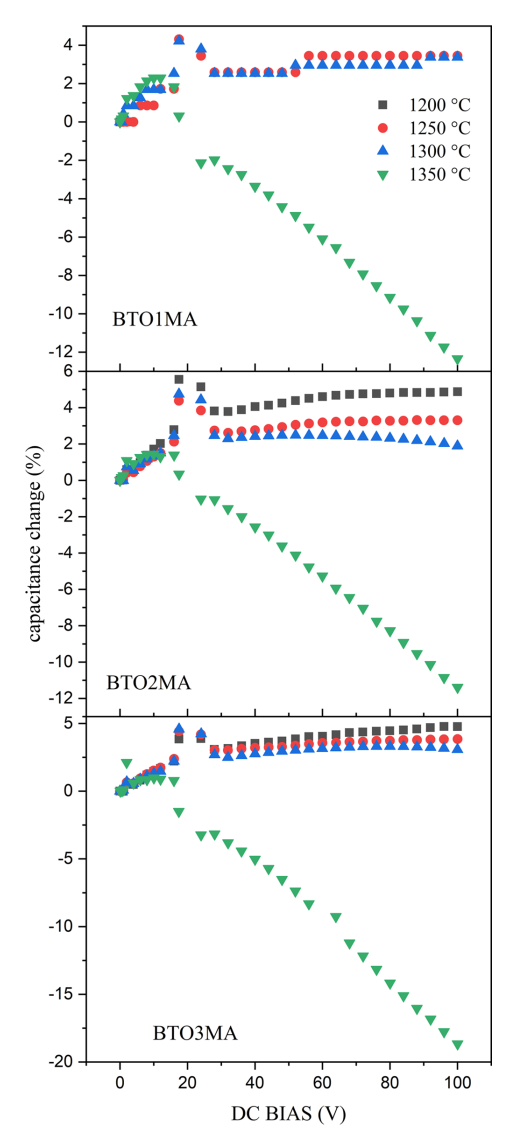


Fig. 9. (Color online) Capacitance change with the applied voltage for BTO samples modified in air.

can show an increase in the capacitance value with the polarization reversal. The problem occurs if a DC bias is applied, completely, or partly preventing spontaneous reversal of polarization due to dipole alignment, which causes a decrease in the capacitance. $^{32}$ 

The change in the capacitance can be expressed using the following equation:

$$CC = \frac{C_E - C_0}{C_0} \times 100\%, \tag{1}$$

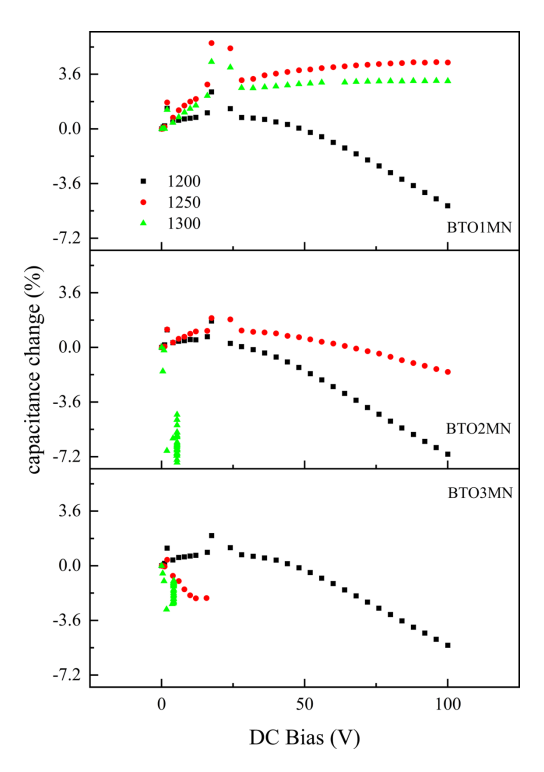


Fig. 10. (Color online) Capacitance change with the applied voltage for BTO samples modified in  $N_2$ .

where  $C_E$  and  $C_0$  stand for capacitance values under and without a DC bias, respectively.

The comparison of DC bias characteristics for the samples sintered in air is presented in Fig. 9. All three samples sintered at  $1200^{\circ}$ C,  $1250^{\circ}$ C and  $1300^{\circ}$ C showed an increase or no change by the influence of the applied voltage, while BTO1MA and BTO2MA sintered at  $1350^{\circ}$ C had moderate decrease of around 12%. BTO3MA sintered at  $1350^{\circ}$ C stands out for the use in capacitors, with high  $D_k$  and an acceptable capacitance drop of 18% at 100 V.

The samples with extremely high  $D_k$  (BTO1MN and BTO2MN) showed great DC bias sensitivity (Fig. 10), which requires further analysis to improve their working stability. Finding optimal sintering parameters to obtain modified BTO with high  $D_k$  and low sensitivity to the applied voltage was achieved through sample BTO3MA sintered at 1350°C. Obviously, organometallic salt offered an efficient shield, resisting dipole orientation under the influence of electric field.

## 4. Conclusion

The high-temperature chemical modification of BaTiO<sub>3</sub> nanoparticles with a yttrium-based salt was performed in order to achieve high dielectric constant

values and DC bias stability. Different sintering temperatures, atmospheres, and nanoparticle sizes were used to investigate the influence of processing parameters on morphological and dielectric properties. The software image analysis of FESEM micrographs was used to emphasize the relation between nanoparticle diameter size, pore size, and porosity. Starting BTO nanoparticle size influenced the pore-size distribution and the ratio of single pores/clusters, which could enable control of the final product by choosing particles of a certain size for the modification. However, the number of pores contributed to the overall porosity of the samples causing the lowest porosity in the BTO3MA sample. The predictions based on image analysis regarding dielectric constant showed that low porosity was the contributing factor to higher  $D_k$  values that were considered high for all the samples. Higher porosity of samples sintered in N<sub>2</sub> suggested that the successful modification of BTO diminished oxygen vacancy generation, thus, leading to an improvement of dielectric properties. The influence of the atmosphere and the modifying agent becomes obvious at the sintering temperature of 1300°C due to the heat-accelerated atom migration. DC bias sensitivity was also strongly dependent on the sintering temperature but the overall behavior of the modified BTO ceramics expresses acceptable capacitance drop where the BTO3MA sample, sintered at 1350°C, was chosen as one of the most optimal candidates considering the high  $D_k$  value of 12,000 and the capacitance drop of 18% at 100 V. The findings presented in this study show that the dielectric properties of chemically modified BTO could be controlled using adequate input parameters. Successful modification of ceramic materials meant to serve as capacitors should lead to a higher dielectric constant and a reduced capacitance drop with the applied voltage, i.e. a higher resistance to a dipole alignment. By varying input synthesis parameters, a trend in the change of dielectric properties can be determined along with the cause. Furthermore, image analysis proved to be a useful tool for predicting dielectric properties, based on morphological characteristics, which opens the way for a thorough characterization of ceramics intended for the application in MLCCs.

## Acknowledgments

This work was financially supported by the Ministry of Education, Science and Technological Development of the Republic of Serbia (Grant Nos. 451-03-68/2022-14/200017 and 451-03-68/2022-14/200026).

## References

- 1. J. Liu, J. Wang, C. Xu, H. Jiang, C. Li, L. Zhang, J. Lin and Z. X. Shen,  $Adv.\ Sci.$  5 (2018) 1700322.
- Q. Li, L. Chen, M. R. Gadinski, S. Zhang, G. Zhang, H. U. Li, E. Iagodkine, A. Haque, L. Q. Chen, T. N. Jackson and Q. Wang, Nature 523 (2015) 576.
- 3. C. Diao, H. Liu, H. Hao, C. Cao, Z. Yao and H. Zheng, Ceram. Int. 44 (2018) 2157.
- 4. L. Zhao, Q. Liu, J. Gao, S. Zhang and J. F. Li, Adv. Mater. 29 (2017) 1.

- R. B. Rakhi, in *Nanocarbon and its Composites*, eds. A. Khan, M. Jawaid and A. M. Asiri (Elsevier, Amsterdam, 2018), pp. 489.
- G. Wang, Z. Lu, H. Yang, H. Ji, A. Mostaed, L. Li, Y. Wei, A. Feteira, S. Sun, D. C. Sinclair, D. Wang and I. M. Reaney, J. Mater. Chem. A 8 (2020) 11414.
- X. Lu, L. Zhang, H. Talebinezhad, Y. Tong and Z. Y. Cheng, Ceram. Int. 44 (2018) 16977.
- 8. S. Pramchu, A. P. Jaroenjittichai and Y. Laosiritaworn, Ceram. Int. 44 (2018) S19.
- 9. Q. Hu, L. Jin, T. Wang, C. Li, Z. Xing and X. Wei, J. Alloys Compd. 640 (2015) 416.
- 10. Z. Shen, X. Wang, B. Luo and L. Li, J. Mater. Chem. A 4 (2016) 18146.
- S. Sharma, M. Tomar, A. Kumar, N. K. Puri and V. Gupta, AIP Adv. 5 (2015) 107216.
- J. Li, K. Inukai, A. Tsuruta, Y. Takahashi and W. Shin, J. Asian Ceram. Soc. 5 (2017) 444.
- 13. M. Zhang, J. Zhai, L. Xin and X. Yao, Mater. Chem. Phys. 197 (2017) 36.
- 14. Z. Yu, C. Ang, R. Guo and A. S. Bhalla, Appl. Phys. Lett. 81 (2002) 1285.
- P. K. Dutta and J. R. Gregg, Chem. Mater. 4 (1992) 843.
- J. Q. Ecker, C. C. Hung-Houston, B. I. Gersten, M. M. Lencka and R. Riman, J. Am. Ceram. Soc. 79 (1996) 2929.
- A. Testino, M. T. Buscaglia, V. Biscaglia, M. Viviani, C. Bottino and P. Nanni, Chem. Mater. 16 (2004) 1536.
- M. Ryu, T. Suzuki, K. Kobayashi, T. Sakashita and Y. Mizuno, Jpn. J. Appl. Phys. 49 (2010) 061101.
- 19. H. Kishi, Y. Mizuno and H. Chazono, Jpn. J. Appl. Phys. 42 (2003) 1.
- F. Le Goupil, A. Baker, F. Tonus, A. Berenov, C. A. Randall and N. M. N. Alford, J. Eur. Ceram. Soc. 39 (2019) 3315.
- 21. H. Gong, X. Wang, S. Zhang and L. Li, Mater. Res. Bull. 73 (2016) 233.
- 22. J. Daniels, *Philips Res. Rep.* **31** (1976) 505.
- 23. D. F. K. Hennings, J. Eur. Ceram. Soc. 21 (2001) 1637.
- 24. J. Boonlakhorn, B. Putasaeng and P. Thongbai, Ceram. Int. 45 (2019) 6944.
- C. L. Freeman, J. A. Dawson, J. H. Harding, L.-B. Ben and D. C. Sinclair, *Adv. Funct. Mater.* 23 (2013) 491.
- 26. V. Paunovic, V. V. Mitic and L. Kocic, Ceram. Int. 42 (2016) 11692.
- 27. S. K. Jo, J. S. Park and Y. H. Han, J. Alloys Compd. 501 (2010) 259.
- 28. Y. A. Zulueta, T. C. Lim and J. A. Dawson, J. Phys. Chem. C 121 (2017) 23642.
- 29. T. Shi, L. Xie, L. Gu and J. Zhu, Sci. Rep. 5 (2015) 8.
- 30. F. D. Morrison, D. C. Sinclair and A. R. West, Int. J. Inorg. Mater. 3 (2001) 1205.
- 31. Q. Liu, J. Liu, D. Lu and W. Zheng, Ceram. Int. 44 (2018) 7251.
- 32. Z. Shen, X. Wang, H. Gong, L. Wu and L. Li, Ceram. Int. 40 (2014) 13833.
- T. Okumura, S. Taminato, T. Takeuchi and H. Kobayashi, ACS Appl. Energy Mater. 1 (2018) 6303.
- Z. Su, Y. Zhang, B. Liu, J. Chen, G. Li and T. Jiang, J. Min. Metall. Sec. B Metall. 53 (2017) 67.
- Z. Liu, Z. Xing, H. Wang, Z. Xue, S. Chen, G. Jin and X. Cui, J. Alloys Compd. 727 (2017) 696.
- 36. M. H. Lin and H. Y. Lu, Mater. Sci. Eng. A 323 (2002) 167.
- J. Jiang, N. Ni, W. Hao, X. Zhao, F. Guo, X. Fan and P. Xiao, J. Eur. Ceram. Soc. 39 (2019) 5332.
- 38. W. G. Yang, B. P. Zhang, N. Ma and L. Zhao, J. Eur. Ceram. Soc. 32 (2012) 899.
- Y. Kuroiwa, S. Kim, I. Fujii, S. Ueno, Y. Nakahira, C. Moriyoshi, Y. Sato and S. Wada, Commun. Mater. 1 (2020) 71.